Near-Infrared Kinetic Spectroscopy of the HO_2 and $C_2H_5O_2$ Self-Reactions and Cross Reactions

A. C. Noell,[†,‡] L. S. Alconcel,[‡,§] D. J. Robichaud,[†,‡,∥] M. Okumura,*[,‡] and S. P. Sander*[,†]

Jet Propulsion Laboratory, California Institute of Technology, 4800 Oak Grove Drive, M/S 183-901, Pasadena, California 91109, and Arthur Amos Noyes Laboratory of Chemical Physics, Division of Chemistry and Chemical Physics, California Institute of Technology, M/S 127-72, 1200 East California Boulevard, Pasadena, California 91125

Received: December 23, 2009; Revised Manuscript Received: April 29, 2010

The self-reactions and cross reactions of the peroxy radicals $C_2H_5O_2$ and HO_2 were monitored using simultaneous independent spectroscopic probes to observe each radical species. Wavelength modulation (WM) near-infrared (NIR) spectroscopy was used to detect HO_2, and UV absorption monitored $C_2H_5O_2$. The temperature dependences of these reactions were investigated over a range of interest to tropospheric chemistry, 221−296 K. The Arrhenius expression determined for the cross reaction, $k_2(T) = (6.01^{+1.95}_{-1.47}) \times 10^{-13} \exp((638 \pm 73)/T)$ cm^3 molecules^{-1} s^{-1} is in agreement with other work from the literature. The measurements of the HO_2 self-reaction agreed with previous work from this lab and were not further refined.[1] The $C_2H_5O_2$ self-reaction is complicated by secondary production of HO_2. This experiment performed the first direct measurement of the self-reaction rate constant, as well as the branching fraction to the radical channel, in part by measurement of the secondary HO_2. The Arrhenius expression for the self-reaction rate constant is $k_3(T) = (1.29^{+0.34}_{-0.27}) \times 10^{-13} \exp((-23 \pm 61)/T)$ cm^3 molecules^{-1} s^{-1}, and the branching fraction value is $\alpha = 0.28 \pm 0.06$, independent of temperature. These values are in disagreement with previous measurements based on end product studies of the branching fraction. The results suggest that better characterization of the products from RO_2 self-reactions are required.

Introduction

The chemistry of alkyl peroxy radicals (RO_2) is central to the oxidation of volatile organic compounds (VOCs) in the atmosphere. In the troposphere RO_2 reacts primarily under two different regimes: high NO_x and low NO_x. Under the high NO_x conditions of urban air RO_2 chemistry contributes to regional air pollution problems by producing O_3. In the unpolluted troposphere ($NO_x < \sim 20$ pptv) the primary loss pathways for RO_2 radicals are self-reaction and cross reaction with HO_2. These reactions lead to the production of organic hydroperoxides (ROOH), which are a temporary reservoir for HO_x. The net effect is to slow down or eliminate the production of O_3 from RO_2 chemistry.[2,3] There is also recent evidence that ROOH and their further reactions are important in the formation of secondary organic aerosol (SOA).[4−6]

Ethane is one of the most abundant non-methane hydrocarbons with a globally averaged annual concentration of ∼1 ppb.[7] The ethyl peroxy radical ($C_2H_5O_2$) is formed in the atmosphere predominantly from the oxidation of ethane

$$C_2H_6 + OH \xrightarrow{O_2} C_2H_5O_2 + H_2O \qquad \text{(R1)}$$

In the remote troposphere the dominant loss process will be reaction with HO_2

$$C_2H_5O_2 + HO_2 \rightarrow C_2H_5OOH + O_2 \qquad \text{(R2)}$$

leading to the formation of ethyl hydroperoxide (C_2H_5OOH). The concentrations of both $C_2H_5O_2$ and HO_2 also depend on their self-reactions

$$C_2H_5O_2 + C_2H_5O_2 \rightarrow \qquad \text{(R3)}$$

$$\rightarrow C_2H_5O + C_2H_5O + O_2 \qquad \text{(R3a)}$$

$$\rightarrow C_2H_5OH + CH_3CHO + O_2 \qquad \text{(R3b)}$$

$$\rightarrow C_2H_5O_2C_2H_5 + O_2 \qquad \text{(R3c)}$$

$$C_2H_5O + O_2 \rightarrow HO_2 + CH_3CHO \qquad \text{(R4)}$$

$$HO_2 + HO_2 \xrightarrow{M} H_2O_2 + O_2 \qquad \text{(R5)}$$

Reaction R4 is a critical link because it leads to the generation of secondary HO_2. This recycles radicals in the atmosphere and complicates laboratory kinetics experiments. The competition between the self-reaction (reactions R3 and R5) and cross reaction (reaction R2) means that a pseudo-first-order kinetics experiment is not possible when trying to measure k_2 and that no analytic solution to the kinetics equations for the reactions exists.

There have been a number of studies of the kinetics[8−13] and products[13−16] of reaction (reaction R2). All of the kinetics studies

* To whom correspondence should be addressed.
† Jet Propulsion Laboratory, California Institute of Technology.
‡ Arthur Amos Noyes Laboratory of Chemical Physics, Division of Chemistry and Chemical Physics, California Institute of Technology.
§ Currently at: Space & Atmospheric Physics Group, The Blackett Laboratory, Imperial College London, Prince Consort Road, London, SW7 2BW, U.K.
∥ Currently at: National Renewable Energy Laboratory, 1617 Cole Blvd, Golden, CO 80401-3305.

10.1021/jp912129j
Published on Web 06/04/2010

with the exception of Cattell et al.[9] and Raventos-Duran et al.[13] used UV absorption alone to monitor peroxy radicals. One problem with UV absorption is that all RO_2 radicals have overlapping broad absorption features arising from a $\pi \rightarrow \pi^*$ transition of the peroxy group. Overlap of the $C_2H_5O_2$ and HO_2 absorption bands requires spectral deconvolution when both radicals are present, increasing the uncertainty of the derived rate coefficient(s). A second problem with UV absorption is that it is not a particularly sensitive method unless long path lengths are used (several meters). This limits the range of initial radical ratios, $[HO_2]_0/[C_2H_5O_2]_0$, that can be used to check for consistency in the kinetics model. A different complication that affected several of the previous temperature-dependent measurements is the use of CH_3OH as a precursor for HO_2.[10,11] It has been demonstrated in this lab and others that CH_3OH acts as a chaperone leading to larger apparent HO_2 self-reaction rate constants at low temperature.[1,16−18] The large variation in the reported range of E_A/R (650−1250 K^{-1}) for reaction R2 is evidence of the difficulties encountered by previous temperature-dependent studies. The product studies on reaction R2 were done with FTIR and chemical ionization mass spectrometry (CIMS), and they show that C_2H_5OOH is the major product.

The self-reaction kinetics of $C_2H_5O_2$ were also measured by a number of groups,[9,11,14,15,19−24] and separate product studies were completed to determine the branching ratios of the different channels.[15,19,25−27] Secondary HO_2 formed through reactions R3a and R4 enhances the apparent rate of reaction for reaction R3, complicating the measurement of k_3. Measuring the disappearance of $C_2H_5O_2$ makes it possible to determine the enhanced rate coefficient k_{3obs}, and from that it is possible to determine k_3 using eq 1 if the branching fraction to the alkoxy channel, α (defined in eq 2), is known.[28]

$$k_3 = \frac{k_{3obs}}{1 + \alpha} \quad (1)$$

$$\alpha = \frac{k_{3a}}{k_3} \quad (2)$$

All of the previous kinetics experiments used UV absorption to measure k_{3obs} and used α from end product studies to determine k_3. The end product studies on reaction R3 are in fair agreement, but there has been no published measurement of α below room temperature. There also has been no measurement of α by a direct observation of the nascent products.

This study aimed to overcome some of the difficulties in previous work by using two probes in different wavelength regions to characterize the above reactions. A near-infrared (NIR) probe measured HO_2 and an ultraviolet (UV) probe measured $C_2H_5O_2$. Experiments were done focusing on either reaction R2 or reaction R3. The rate coefficient k_2 was measured during experiments on reaction R2. In the experiments focusing on reaction R3, UV detection of $C_2H_5O_2$ allowed for the determination of k_{3obs} similar to previous studies. In addition, the NIR measured the time profile of secondary HO_2 from reactions R3 and R4 allowing for real time determination of α and k_3 for the first time. The measurements made of each reaction were then used together to develop a self-consistent description of the self-and cross reactions of $C_2H_5O_2$ and HO_2.

Experimental Section

A. Summary. A detailed description of the experimental apparatus has been given previously.[29] The IRKS apparatus consisted of a flash photolysis flow cell coupled with two optical probes for time-resolved HO_2 and $C_2H_5O_2$ detection. A XeCl excimer laser created a column of radicals down the length of the ∼2 m flow cell. $C_2H_5O_2$ was detected by UV absorption spectroscopy. The UV light from a deuterium lamp was coupled into the cell along the same path as the excimer but in a counterpropagating direction. A monochromator was used to select the desired wavelength from the light exiting the cell. HO_2 was detected at the overtone of its OH stretching vibration using NIR wavelength modulation (WM) spectroscopy. The NIR light was also coupled in lengthwise but was slightly off axis compared to the excimer and deuterium lamp. The NIR beam began above and ended below the deuterium and excimer beams, but made 30 passes crossing through the photolysis region in a Herriott cell setup. Data acquisition was gated to the firing of the excimer, and data for both optical probes were recorded simultaneously. The data from both probes were then fit simultaneously to determine the desired kinetics parameters.

B. Apparatus and Detection Probes. The radical chemistry took place in a 175 cm long, 5 cm diameter reaction cell. The intersection of the reactant gases with the excimer laser defined the photolysis volume, 2 cm × 1 cm × 148 cm. The gas flows were adjusted so that the residence time in the flow cell (typically 10−15 s) matched the interval between photolysis laser pulses. Photolysis of Cl_2 by a XeCl excimer laser (308 nm, 110 ± 15 mJ/pulse) led to the formation of HO_2 and $C_2H_5O_2$ by the reaction sequence

$$Cl_2 + h\nu(308\ nm) \rightarrow 2Cl \quad (R6)$$

$$\begin{aligned} Cl + CH_3OH &\rightarrow CH_2OH + HCl \\ Cl + C_2H_6 &\rightarrow C_2H_5 + HCl \end{aligned} \quad (R7)$$

$$\begin{aligned} CH_2OH + O_2 &\rightarrow HO_2 + HCHO \\ C_2H_5 + O_2 &\xrightarrow{M} C_2H_5O_2 \end{aligned} \quad (R8)$$

For the experiments on the $C_2H_5O_2$ self-reaction, no CH_3OH was used, but there is a small source of HO_2 from the reaction that forms $C_2H_5O_2$.

$$C_2H_5 + O_2 \rightarrow HO_2 + C_2H_4 \quad (R9)$$

The HO_2 concentration resulting from reaction R9 was measured to be ∼1% of the initial $C_2H_5O_2$. This value is in good agreement with previous work by Kaiser et al. but is slightly higher than new measurements by Clifford et al.[30−32]

The temperature in the cell was held to within ±1 K of the stated temperatures. Methanol cooled by liquid nitrogen circulated through a jacket around the cell to obtain temperatures below 298 K. Calibrated flows of reagent gases were cooled and mixed in a 1 m long tube before flowing into the middle of the reaction cell. The temperature inside the cell was measured with a type T thermocouple (Omega). A purge flow was used to protect the NIR Herriott mirrors from corrosion and contain the main flow to the temperature-controlled region. The mixing of the purge flow and reactant gases occurred throughout 10 cm on either side of the cell leading to a path length of 148 ± 10 cm.

Typical reagent gas concentrations were, in units of molecules cm^{-3}: Cl_2, (0.3−1.5) × 10^{16}; He, (3−15) × 10^{16}; CH_3OH,

(0−2.5) × 10^{15}; C_2H_6, (0.5−30) × 10^{15}, O_2: (5−20) × 10^{17}; N_2, (0−1) × 10^{18}. The CH_3OH was carried into the cell by N_2 after it passed through the liquid CH_3OH (J.T. Baker, PHOTOREX Reagent) in a bubbler held at 273 K. The experiments on the cross reaction (R2) were performed in O_2. The $C_2H_5O_2$ self-reaction (R3) measurements were primarily in O_2 as well, but used N_2 as a buffer when investigating the effect of varying O_2 concentrations on α. All gas flows were monitored with mass flow meters (Hastings HFM-200 series) and controlled with needle valves. Sufficient concentrations of C_2H_6 and/or CH_3OH were always used to ensure stochiometric conversion of Cl to either $C_2H_5O_2$, HO_2, or both. In the experiments on (R2) flows were adjusted to investigate the kinetics over a wide range of initial radical ratio: $[HO_2]_0/[C_2H_5O_2]_0$. This ratio typically ranged from 0.1 to 4 while the total concentration of radicals remained constant at ∼1 × 10^{14} molecules cm^{-3}. For experiments on reaction R3 the total radical concentration was varied, typically from 3.0 × 10^{13} to 1.5 × 10^{14} molecules cm^{-3}. At least six measurements were made spaced throughout the range of the initial radical ratio, or total radical concentration, at every temperature and pressure for (R2) and (R3), respectively. The pressures in the cell and the CH_3OH bubbler were monitored by capacitance manometers (MKS-220CA 1000 Torr) and were constant within ±2 Torr of the stated pressures. Flow meters were calibrated by measuring the time required to flow through a calibrated volume over a range of flows suitable to each meter. The capacitance manometers were calibrated in reference to other factory calibrated capacitance manometers.

Two optical probes were used to monitor the radical chemistry. The UV light source was a 150 W deuterium lamp (Hamammatsu L1314). The beam made a single pass through the cell counterpropagating with the excimer photolysis beam. Baffles on either end of the reaction cell ensured that only light that had sampled the photolysis region entered the monochromator slit. The monochromator was set to 250.0 nm for detection of $C_2H_5O_2$. The minimum detectable absorbance for $C_2H_5O_2$ was ∼2 × 10^{-5} $Hz^{-1/2}$ (∼6 × 10^{12} molecules cm^{-3}). The monochromator was calibrated against atomic emission lines from a Hg pen lamp. The NIR probe source was a 3 mW distributed-feedback (DFB) continuous-wave tunable diode laser manufactured in the JPL Microdevices Laboratory. The laser was tuned for HO_2 at the $^qQ_2$ band head (6638.2 cm^{-1}) of the first overtone of the OH stretch.[33] The NIR beam made 30 passes through the reaction cell using a Herriott cell setup with an estimated effective path length of 2700 cm. The laser was wavelength modulated at 6.8 MHz by varying the drive current with an external rf generator. The signal from the InGaAs photodiode detector (New Focus 1811) was demodulated at 13.6 MHz (2f detection) and subsequently amplified by a factor of 100. The minimum detectable absorbance for HO_2 was ∼2 × 10^{-7} $Hz^{-1/2}$ (∼ 1 × 10^{11} molecules cm^{-3}).

The detector signals for both optical probes were recorded simultaneously. The data acquisition was controlled by a Visual BASIC program. For reaction R2 the decay measurements typically began 1 ms before the excimer fired to establish a baseline for the signal, and continued for 20 ms at a sampling rate of 200 kS/s. For reaction R3 the baseline was recorded for 10 ms before the excimer pulse and continued for 200 ms at a sampling rate of 20 kS/s to capture the slower decay. Both signals were low pass filtered at 100 and 10 kHz, respectively (SRS-SR560). The data were digitized using a two channel 16 bit per channel A/D card with a maximum sampling rate of 2.5 MS/s (Gage-CompuScope 1602). Decay traces for the UV and the IR probes were obtained by averaging the signals over 50 excimer shots.

C. Calibration of the NIR Probe. The NIR probe was calibrated daily to measure HO_2 because WM spectroscopy measures relative, not absolute, changes in concentration. The NIR probe was calibrated with the UV absorption probe by measuring the kinetics of the HO_2 self-reaction (R5). The two probe beams measure the same physical processes, albeit with different geometrical overlap, but should yield the same bimolecular kinetics at short time scales (∼20 ms). At the beginning of each day, data for reaction R5 were taken where the only peroxy radical present was HO_2. The UV monochromator was set to 220.0 nm to monitor HO_2 at the same as it was monitored by the NIR. The time decays of both probes were fit simultaneously with the kinetics modeling program FACSIMILE.[34] The fits checked for consistency between the probes and determined that day's calibration factor for the NIR. The rate coefficient of the HO_2 self-reaction k_5 used in the kinetic modeling of reactions R2 and R3 was taken from these daily measurements as it was determined along with the value of the calibration factor for the NIR. This calibration factor was very sensitive to optical alignment but, in general, was consistent from day to day within ±15%. The UV detection wavelength was then optimized for $C_2H_5O_2$ detection to allow for the simultaneous independent detection of both radicals.

D. Diffusion and Transport Loss. The effect of losses from diffusion and transport for this apparatus has been previously described,[29] but is discussed here in the context of the slower ethyl peroxy radical self-reaction. For reactions that were complete in <20 ms, diffusion and transport losses had a negligible effect, but all data were treated the same way. Overall, the model of the UV data included an explicit unimolecular loss term describing the diffusion and transport, but the NIR model did not because of offsetting effects.

The UV was coaligned with the excimer laser down the middle of the flow cell. The radicals created down the middle of the cell diffused radially out of the UV beam given sufficient time. This type of diffusion was approximated as a unimolecular loss term in the kinetic fits. By variation of the initial concentration of total radicals and determination of the observed bimolecular rate coefficient, the contribution of diffusion to the observed rate coefficient was determined in the manner of Thiebaud et al.[35]

The NIR was complicated by the geometry of the Herriott cell. The NIR beam passed in and out of the photolysis region because of its off axis alignment with respect to the excimer. Diffusion allowed parts of the beam originally outside the photolysis region to interact with radicals and extend the path length. However the concentration profile along that path length was not uniform. The different concentrations underwent reaction at different rates. At longer times as more and more of the beam passed through smaller concentrations of the radical, the bimolecular reaction rate appeared to have slowed down. The apparent slowing of the bimolecular rate and the lengthening of the path compensate for any loss due to diffusion, so no diffusion was modeled. However the effects are not perfectly offsetting and led to a small systematic residual in the IR signal. This effect on the overall error analysis will be discussed in the results and analysis section.

Results and Analysis

A. Overview. Reactions R2 and R3 were the primary focus of this work. Perfect isolation of each reaction is not possible because they are connected by secondary chemistry. In order

TABLE 1: Reactions Used in Kinetics Model Fits

reaction	k_{298}[a]	
$HO_2 + C_2H_5O_2 \rightarrow C_2H_5OOH + O_2$	$5.5 \pm 0.4 \times 10^{-12}$	k_2[b]
$C_2H_5O_2 + C_2H_5O_2 \rightarrow 2C_2H_5O_2 + O_2$	$2.3 \pm 1.1 \times 10^{-14}$	k_{3a}[b]
$\rightarrow C_2H_5OH + CH_3CHO + O_2$	$1.0 \pm 0.1 \times 10^{-13}$	k_{3b}[b]
$C_2H_5O + O_2 \rightarrow HO_2 + CH_3CHO$	1.0×10^{-14}	k_4[c]
$HO_2 + HO_2 \xrightarrow{M} H_2O_2 + O_2$	1.7×10^{-12}	k_5[b]
$C_2H_5O_2 + C_2H_5O \rightarrow C_2H_5OOH + CH_3CHO$	$1.5 \pm 0.7 \times 10^{-11}$	k_{10}[b]
$C_2H_5O_2 \xrightarrow{\text{diffusion, UV}}$	$5 \pm 1\ s^{-1}$	k_D[b]
$HO_2 \xrightarrow{\text{diffusion, UV}}$	$5 \pm 1\ s^{-1}$	k_D[d]

[a] Units of cm^3 molecules^{-1} s^{-1} except where explicitly written. [b] Determined during present work. [c] Reference 36. [d] Used $C_2H_5O_2$ value.

to achieve the greatest sensitivity to k_2 and k_3 separately, two types of experiments were performed: one type in which both HO_2 and $C_2H_5O_2$ were created deliberately, and a second type where only $C_2H_5O_2$ was created deliberately. Both types of experiments were done using simultaneous NIR and UV probes of HO_2 and $C_2H_5O_2$, respectively. The rate coefficients k_2 and k_3 and the branching fraction α were measured in a self-consistent manner. Correlation among the parameters was explored and accounted for throughout the data analysis.

B. Methods and Error Analysis. All three of the major kinetics parameters determined in this study (k_2, k_3, and α) could not be well determined at the same time. Nonphysical values for the parameters were returned when all three were varied at once. Therefore it was necessary to follow an iterative procedure for fitting the data. First the NIR was calibrated with data from reaction R5 as described in the Experimental Section on NIR calibration. Data for reaction R2 with $[HO_2]_0/[C_2H_5O_2]_0 > 1$ (typically three different conditions) were then fit in order to approximate k_2. Secondary chemistry from reaction R3 does not interfere when HO_2 is in excess because k_2 is ∼50 times larger than k_3, and almost all $C_2H_5O_2$ will react with HO_2. The estimate for k_2 was then used in fits of the (R3) data to give values for k_3 and the branching fraction α. The values for k_3 and α were then used to fit the rest of the reaction R2 data where $[HO_2]_0/[C_2H_5O_2]_0 \leq 1$. Under these conditions the secondary chemistry of (R3) has an effect on the values obtained for k_2. A new value of k_2 was obtained by averaging the values from all of the fits of (R2) data. This value of k_2 was then used in subsequent fits of (R3) data, and all of the values were refined iteratively. In practice two iterations were sufficient to achieve convergence. Table 1 presents the full chemical model used while fitting the reactions and what parameters were fit. All fits were performed using the program FACSIMILE.[34] Data fitting started at 200 μs after the photolysis laser pulse for both reactions. The (R2) data were typically fit to 5−10 ms. The data for the slower (R3) were fit out to two half-lives (50−200 ms) in order to account for the varying values of $[C_2H_5O_2]_0$. In all fits the radical source chemistry was neglected and the initial radical concentrations $[HO_2]_0$ and $[C_2H_5O_2]_0$ were fit as well. The initial radical concentrations from the fits were consistent with the ratios of $[CH_3OH]$ and $[C_2H_6]$, the precursors of HO_2 and $C_2H_5O_2$, respectively.

Sample fits with residuals for both (R2) and (R3) are shown in Figure 1. In parts A and B of Figure 1 are the data and fits for (R2) at 273 K, 50 Torr, and $[HO_2]_0/[C_2H_5O_2]_0 = 1.13$ in the NIR and UV, respectively. The high signal-to-noise ratio for the HO_2 NIR signal reveals the subtle systematic residual attributed to diffusion and described in the calibration of the NIR probe portion of the experimental section. Parts C and D of Figure 1 show the NIR and UV traces for reaction (R3) taken at 273 K, 50 Torr, and 8.8×10^{13} molecules cm^{-3} total radicals. At the HO_2 concentrations in Figure 1C (∼100 times lower than those in Figure 1A) the diffusion effect is masked by the signal noise. For both (R2) and (R3) the fits agree well with the UV and NIR signals.

By setting the monochromator to 250.0 nm, the ratio of $C_2H_5O_2$ and HO_2 cross sections was maximized at ∼9:1 ($C_2H_5O_2$, $\sigma = 4.1 \times 10^{-18}$ cm^2; HO_2, $\sigma = 0.48 \times 10^{-18}$ cm^2)[36] within the operating wavelength range of the experiment. The peroxide products of (R2) and (R5), C_2H_5OOH and HOOH, respectively, also absorb at 250 nm. The absorption cross section for C_2H_5OOH has not been measured but was assumed to be the same as that for CH_3OOH. We make this assumption because the hydroperoxides all share a broad dissociative transition in the UV (210−365 nm) due to the breaking of the O−O bond.[37] While σ_{250} values for HOOH and CH_3OOH vary by a factor of 2, the values for CH_3OOH and HOCH2OOH are virtually identical suggesting that differences past the α atom will not have a large influence on cross section. The values used for HOOH and C_2H_5OOH at 250 nm are $\sigma = 8.3 \times 10^{-20}$ and $\sigma = 3.98 \times 10^{-20}$ cm^2, respectively.[36]

The uncertainties stated in the following sections come from random error and systematic error. The random errors are accounted for in a straightforward way by determining the standard deviation from the mean. The mean was determined by averaging values of k_2, k_3, and α from runs at the same temperature and pressure but with different initial radical ratios or total radical concentrations, respectively. (At least six measurements were averaged in each case.) One potential source of systematic error was the uncertainty from the fitting procedure just described. In the initial fits to the data for (R2) where $[HO_2]_0/[C_2H_5O_2]_0$ was high, the low signal-to-noise ratio in the UV detection of $C_2H_5O_2$ and the small systematic residual in the NIR detection of HO_2 led to a range of acceptable fits and a range in the value for k_2. The quality of the fits was determined by the overall residual sum of squares as well as by visual evidence of nonrandom residuals. The high and low values for k_2 were then propagated through the fitting routine in order to determine the effect of this uncertainty on the values of k_3 and α. The values of k_3 and α returned, but not the overall quality of the fits, relied on the value of k_2 used to fit them. This meant a range of k_2 values led to similarly high-quality fits to the data

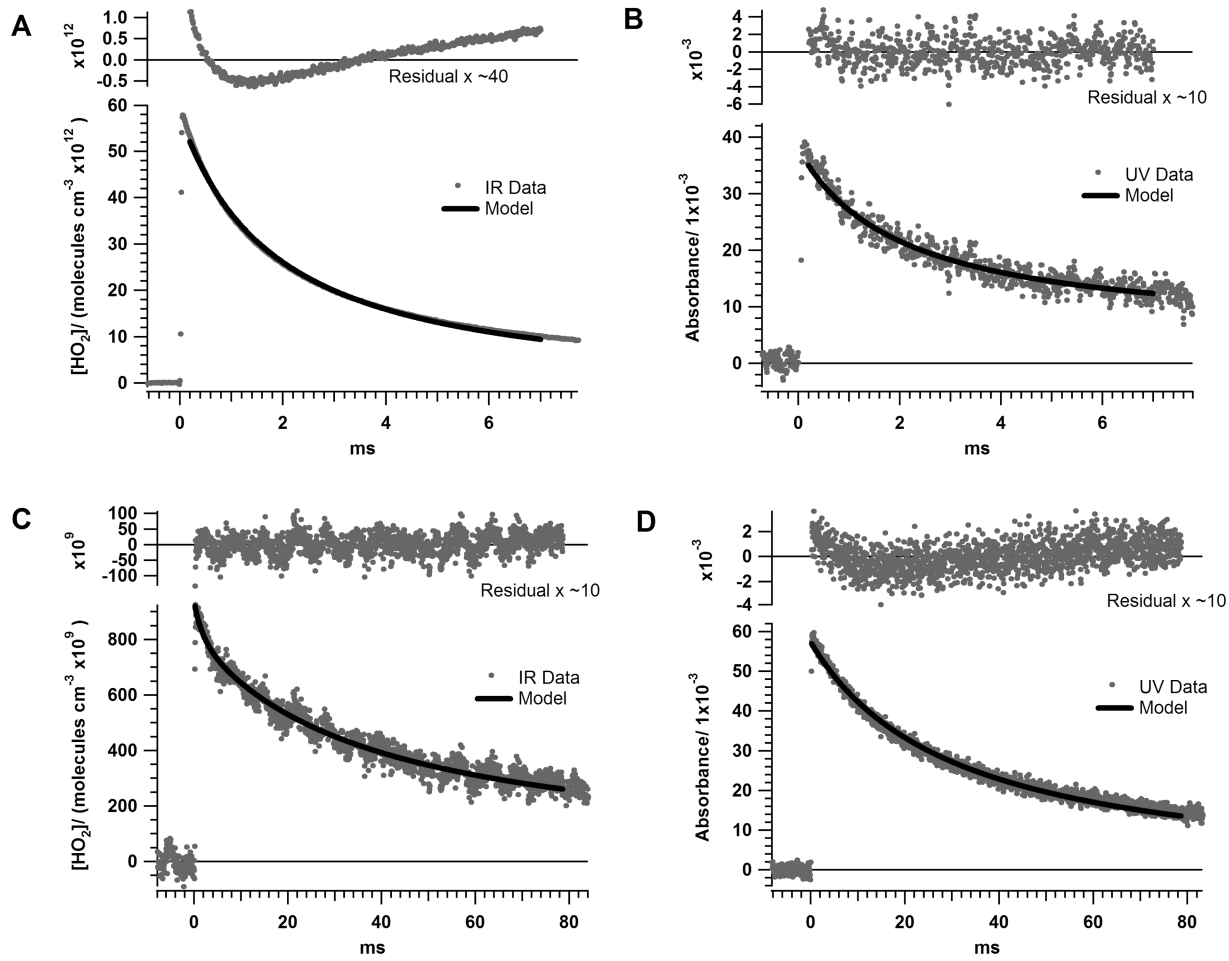

Figure 1. (A) Example fit of NIR data with residual for (R2). (B) Example fit of UV data with residual for (R2). The data were taken at 273 K, 50 Torr, $[CH_3OH] = 4 \times 10^{15}$ molecules cm^{-3}, and $[C_2H_5O_2]_0$:$[HO_2]_0 = 1.13$. (C) Example fit of NIR data with residual for (R3). (D) Example fit of UV data with residual for (R3). The data were taken at 273 K, 50 Torr, and 8.8×10^{13} molecules cm^{-3}.

from (R3), but returned a proportional variety in values for k_3 and α. The uncertainty in the k_2 fits and the correlating uncertainties in k_3 and α were smaller than the random uncertainties but not negligible. Both sources of error were combined in quadrature. An example of these 1σ error bars at two temperatures for k_2 are shown in Figure 2 and show how the overall uncertainties get larger at $[HO_2]_0/[C_2H_5O_2]_0 > 1$ due to increased uncertainty in the fits.

The major source of systematic error was the uncertainty in the path length due to the mixing of the purge and reactant gas flows. To determine the error associated with this uncertainty, the data were analyzed at the maximum and minimum possible lengths, i.e., 138 and 159 cm. Upper and lower error bounds were determined by applying the random and fitting uncertainties just discussed to these analyses at the long and short path length. The total error determined in this way was considered a 2σ error bar. The final errors are reported as half this at their 1σ limits.

These are the error bars displayed with data presented in Figures 4, 5, and 6 and in Tables 3 and 4. The uncertainties do not take into account the error associated with σ for HO_2 and $C_2H_5O_2$ in the UV.

Another potential contributor to the error from reaction R3 is the correlation among the measured parameters k_3 and α. Unlike the correlation between k_2, k_3, and α just described, k_3 and α are impossible to determine independently in this experiment. Fortunately the quality of the fit to the data degrades rapidly if k_3 or α is fixed away from their simultaneously fit values. This meant that the contribution to the overall error was much smaller than the random error and was not included. Figure 3 compares fits that use the JPL-06 ($\alpha = 0.6$), the data fit ($\alpha = 0.28$), and an arbitrary lower value ($\alpha = 0.10$) for α and provides an example of how fits to the data do not capture the behavior observed when k_3 and α are not fit simultaneously. The NIR HO_2 data in Figure 3A show clearly that the JPL-06

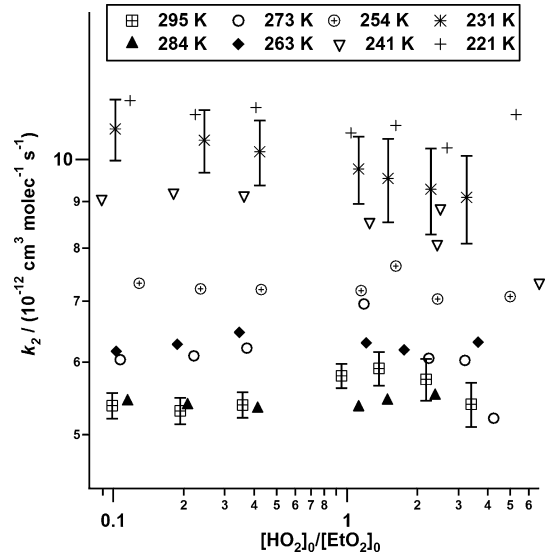

Figure 2. Plot of k_2 vs $[HO_2]_0/[C_2H_5O_2]_0$ for T 221−296 K. Error bars are examples of data precision.

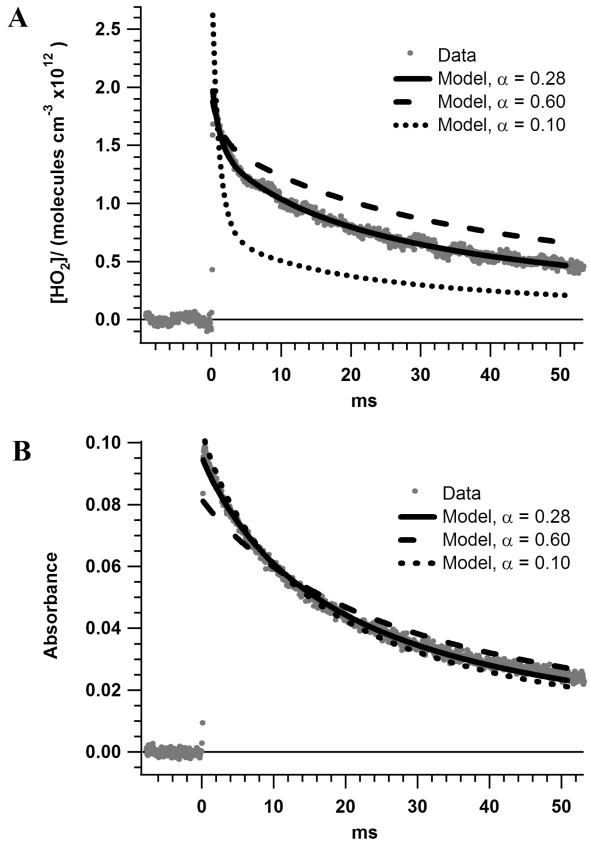

Figure 3. (A) Example of NIR data for (R3) while holding α at three different values and the effect it produces on the fit. (B) Example of UV data for (R3) while holding α at three different values and the effect it produces on the fit. By fixing α away from the middle value actually determined, one or both fits in the NIR and UV no longer fit the data.

value for α predicts larger concentrations of HO_2 than are observed and that the lower value predicts much lower concentrations. In Figure 3B the fit to the UV data that largely determines k_3 shows a much slower rate constant for the JPL-06 and faster one for the lower α value. Figure 3 demonstrates that although k_3 and α are correlated, pulling one away from its best fit value also pulls the other away from its best fit.

C. HO_2 + $C_2H_5O_2$ Rate Coefficient. Measurements of the rate coefficient k_2 were performed over the temperature range 221−296 K and the pressure range 50−200 Torr. For each combination of temperature and pressure, the initial radical ratio ($[HO_2]_0/[C_2H_5O_2]_0$) was varied over the range 0.1−3. The ranges of initial radical concentrations were as follows, in units of molecules cm^{-3}: $[HO_2]_0$, (0.1−1) × 10^{14}; $[C_2H_5O_2]_0$, (0.3−1) × 10^{14}. Figure 2 shows the values obtained for k_2 vs $[HO_2]_0/[C_2H_5O_2]_0$ at each temperature at a pressure of 50 Torr. For clarity error bars have only been included for 295 and 231 K. Figure 4 shows a comparison of the current work to previous studies at temperatures ≤298 K. Table 2 lists the values of k_2 measured in this study. The values of k_2(298 K) and the Arrhenius parameters for all of the studies are given in Table 3. An Arrhenius fit to our data gives the expression

$$k_2(T) = (6.01^{+1.95}_{-1.47}) \times 10^{-13} \exp\left(\frac{638 \pm 73}{T}\right) \text{cm}^3 \text{ molecules}^{-1} \text{ s}^{-1}$$

The pressure dependence of k_2 was studied over the range 50−200 Torr of N_2 at 296 and 231 K. No dependence on pressure was observed at either of these temperatures in agreement with previous measurements.[9,10,12,13]

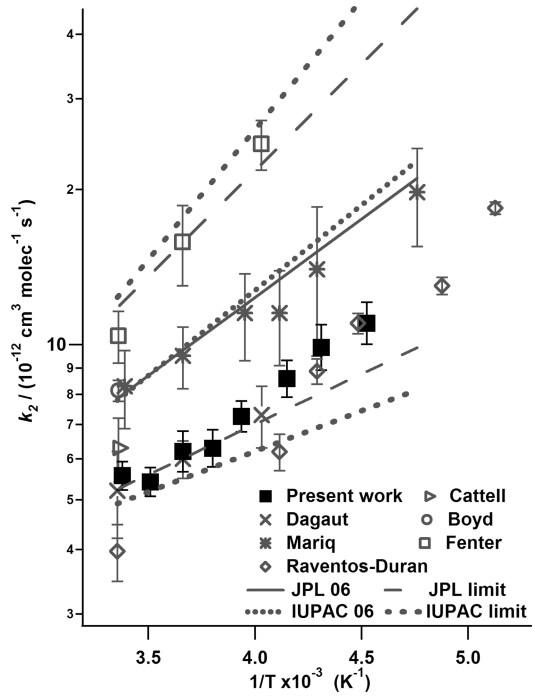

Figure 4. Comparison of k_2 for the HO_2 + $C_2H_5O_2$ cross reaction with previous work. Error bars are 1σ.

TABLE 2: Measured Rate Coefficient for HO_2 + $C_2H_5O_2$

T (K)	$k_2/10^{-12}$ [a]
295	5.57 ± 0.36
284	5.41 ± 0.36
273	6.20 ± 0.59
263	6.29 ± 0.54
254	7.25 ± 0.52
241	8.59 ± 0.74
231	9.87 ± 1.06
221	11.0 ± 1.08

[a] Units cm^3 $molecules^{-1}$ s^{-1}.

TABLE 3: Summary of Results for the HO_2 + $C_2H_5O_2$ Reaction Rate Constant

ref	$A/10^{-13}$ [a]	$-E_a/R$ (K^{-1})	k_2(298 K)/10^{-12} [a]
9	NA	NA	6.3
10	5.6 ± 2.4	650 ± 125	5.2
11	1.6 ± 0.4	1260 ± 130	10.4
12	6.9 (+2.1, −1.6)	702 ± 69	8.3
8	NA	NA	8.14
13	2.08 (+0.87, −0.62)	864 ± 79	3.97
b	**6.01 (+1.95, −1.47)**	**638 ± 73**	**5.6**

[a] Units of $molecules^{-1}$ cm^3. [b] Present work.

D. $C_2H_5O_2$ + $C_2H_5O_2$ Kinetics and Branching Fraction. Three kinetics parameters were determined from the studies of (R3): k_{3obs}, k_3, and α. Reaction R3 was investigated over the same temperature range as (R2), 221−296 K. The total initial radical concentration was varied over the range 3.0 × 10^{13} to 1.5 × 10^{14} molecules cm^{-3}. At the largest total radical concentrations, $[O_2]$ was varied to check for secondary chemistry other than the production of HO_2. Using the UV data alone, it is possible to determine k_{3obs}, which is related to k_3 by eq 1. The value of k_{3obs} measures the total loss of $C_2H_5O_2$. It incorporates loss both from the self-reaction and from reaction with secondary HO_2. Combining the UV and NIR data allows

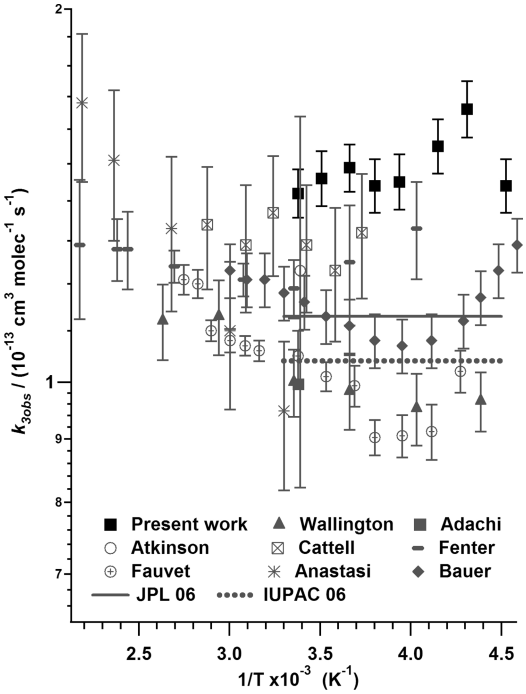

Figure 5. Comparison of k_{3obs} for the $C_2H_5O_2$ self reaction with previous work. Error bars are 1σ.

for determination of k_3 and α. Values for k_{3obs} were measured over the pressure range 50−200 Torr. Values for k_3 and α could only be measured at 50 Torr because of decreased sensitivity due to pressure broadening in the WM detection of HO_2.

It is difficult to directly compare the different values of k_{3obs} from different studies because the value actually measured, k_{3obs}/σ_λ, is dependent on the wavelength used to make the determination and the spectrometer instrument line shape function. In the present study to determine k_{3obs}, $\lambda = 250$ nm was used and σ_{250} was taken from the JPL-06 recommendation.[36] In order to compare with the present work, previous data sets were normalized to the value of σ recommended in the JPL-06 evaluation for the λ used in that experiment. Figure 5 compares the previous and present work on k_{3obs}. An Arrhenius fit to our data leads to the expression

$$k_{3obs}(T) = (1.18^{+0.23}_{-0.19}) \times 10^{-13} \exp\left(\frac{58 \pm 45}{T}\right) \text{cm}^3 \text{ molecules}^{-1} \text{ s}^{-1}$$

Table 4 presents our data for k_{3obs} at all temperatures and pressures. We do not see a pressure dependence for k_{3obs} in agreement with previous results; however, there is a slightly anomalous decrease in k_{3obs} at 200 Torr. Values for k_d, the rate coefficient for the unimolecular disappearance due to diffusion, were determined along with the values for k_{3obs}. For $C_2H_5O_2$, $k_d = 5 \pm 1$ s^{-1} and was invariant over the pressure range 50−200 Torr. Diffusion coefficients should be inversely proportional to pressure, so if rather than using the measured value we assume a linear dependence on pressure (i.e., if $k_d = 5$ s^{-1} at 50 Torr, then at 200 Torr $k_d = 1.25$ s^{-1}) and use that to fit the 200 Torr data, we get values for k_{3obs} that agree much better. These values are shown in parentheses for the 200 Torr data in Table 4. While it cannot be ruled out that the lower pressure data are underrepresenting the diffusion effect, this seems unlikely because the fits to the 200 Torr data improve based on total residual sum of squares when using the lower k_d values. Trying the opposite route, increasing k_d for the 50 Torr data

TABLE 4: Results of $C_2H_5O_2$ Self-Reaction

T (K)	P (Torr)	$k_{3obs}/10^{-13}$ [a]	$k_3/10^{-13}$ [a]	α
295	50	1.42 ± 0.07	1.10 ± 0.09	0.32 ± 0.05
284	50	1.46 ± 0.08	1.17 ± 0.07	0.27 ± 0.03
273	50	1.49 ± 0.07	1.22 ± 0.05	0.23 ± 0.03
263	50	1.44 ± 0.07	1.18 ± 0.06	0.23 ± 0.03
254	50	1.45 ± 0.08	1.13 ± 0.06	0.30 ± 0.03
241	50	1.55 ± 0.08	1.24 ± 0.07	0.28 ± 0.03
231	50	1.66 ± 0.09	1.36 ± 0.11	0.25 ± 0.05
221	50	1.44 ± 0.07	1.02 ± 0.07	0.43 ± 0.05
295	200	1.20 ± 0.09 (1.55)		
231	200	1.23 ± 0.09 (1.62)		
298[b]	all P	1.1	6.8	0.6
298[c]	all P	1.0	6.4	0.62

[a] Units cm^3 molecule^{-1} s^{-1}. [b] Values from ref 36. [c] Values from ref 39.

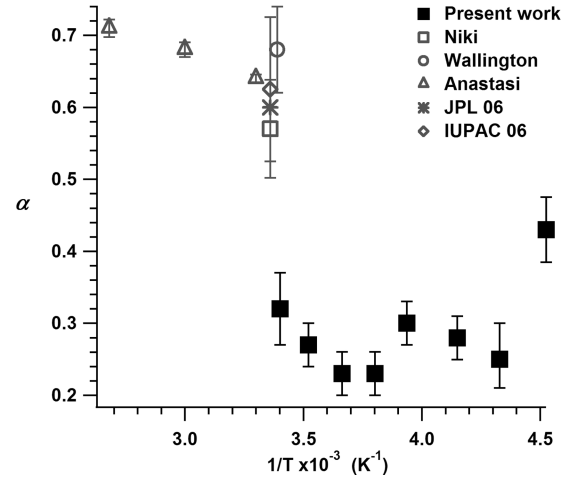

Figure 6. Comparison of α with previous work. Error bars are 1σ. Previous studies were all done on the time scale of minutes after the reaction, whereas the current work monitored the secondary HO_2 production on the time scale of the reaction (micro-milliseconds).

linearly (i.e., 50 Torr $k_d = 20$ s^{-1}) from the fitted 200 Torr values, leads to unacceptable fits.

The values for α are shown in Figure 6 along with the previous results from the end product studies. To our knowledge this is the first published investigation of the temperature dependence of α for $C_2H_5O_2$ below room temperature. A weighted average of the measurements leads to the expression $\alpha = 0.28 \pm 0.06$. The larger error bars and scatter of the measured value reflect the sensitivity of α to correlation with the other parameters but were not interpreted as any temperature dependence.

For reaction R3 varying the $[O_2]$ provided a check on whether (R4) was the only subsequent reaction of C_2H_5O. In our experiments where $[O_2]$ was varied, no difference in k_{3obs} was measured similar to the experiments of Cattell et al.[9] However values for α did not remain consistent as $[O_2]$ varied, and the temporal profile of HO_2 from the IR data could not be fit as accurately. Inclusion of the chemistry suggested by Cattell et al.

$$C_2H_5O_2 + C_2H_5O \rightarrow C_2H_5OOH + CH_3CHO \quad \text{(R10)}$$

allowed for agreement across all $[O_2]$ values. Values for k_{10} were generally determined at the lowest $[O_2]$ values where (R4) would be slowed; under these conditions we measured, $k_{10} =$

$(1.54 \pm 0.7) \times 10^{-11}$ cm^3 molecules^{-1} s^{-1} independent of temperature. Other competing reactions were considered as well, but no other reactions had a significant impact on the results. One example is the reaction of HO_2 with C_2H_5O, but even assuming a fast rate coefficient of 1.0×10^{-10} cm^3 molecules^{-1} s^{-1}, it only changed measured values for k_2, k_3, and α by <1%. This is because HO_2 reacts faster with $C_2H_5O_2$ than $C_2H_5O_2$ does with itself to produce the C_2H_5O, so whenever concentrations of HO_2 are large, concentrations of C_2H_5O are small.

Lastly it was possible to measure k_3 directly. The Arrhenius expression derived from the data is

$$k_3(T) = (1.29^{+0.34}_{-0.27}) \times 10^{-13} \exp\left(\frac{-23 \pm 61}{T}\right) \text{cm}^3 \text{ molecules}^{-1} \text{ s}^{-1}$$

Table 4 shows the values measured for k_{3obs}, k_3, and α along with current recommendations for them.

E. CH_3OH Chaperone Effect. The methanol chaperone effect on reaction R5 has previously been investigated in this laboratory and others.[1,16] This effect enhances the observed rate of reaction at low temperatures through the following mechanism.

$$HO_2 + CH_3OH \rightleftharpoons HO_2 \bullet CH_3OH \qquad \text{(R11)}$$

$$HO_2 \bullet CH_3OH + HO_2 \rightarrow H_2O_2 + O_2 + CH_3OH \qquad \text{(R12)}$$

Net:

$$HO_2 + HO_2 \xrightarrow{CH_3OH} H_2O_2 \qquad \text{(R13)}$$

Under the conditions of low $[CH_3OH]$ used in this experiment, the dependence of k_{5obs} on $[CH_3OH]$ is that derived in the Christensen et al. paper[38]

$$k_{5obs} = k_5 + (k_{12} - 2k_5)K_{11}[CH_3OH] \qquad (3)$$

In this experiment it was investigated whether the HO_2•CH_3OH complex might change the observed kinetics of (R2). At 241 K, a set of experiments at $[CH_3OH]$ of 1×10^{15}, 2.5×10^{15}, and 5×10^{15} molecules cm^{-3} were performed. No evidence for a methanol chaperone effect was observed on (R2) at the conditions studied. We were unable to investigate this effect further at lower temperatures and/or higher $[CH_3OH]$ due to the large amount of complex that is formed under those conditions. When >∼10% of the HO_2 exists in a complexed state, the UV and NIR spectroscopies in this experiment are no longer observing the same simple bimolecular reaction. This makes it difficult to accurately calibrate the NIR probe signal. A comprehensive study including other low temperatures and investigating the effect of H_2O would be valuable but was outside the scope of the present work.

This work, and the daily calibration of the NIR probe during which k_5 was measured, also showed that our measurements of k_5 agreed with those previously determined by Christensen et al. in the same laboratory.[1]

Discussion

The major strength of this experiment was the ability to monitor HO_2 and $C_2H_5O_2$ using simultaneous but distinct optical probes in the NIR and UV, respectively. A self-consistent method was used for measuring the interrelated parameters k_2, k_3, and α. For the first time α was determined by measurement of the nascent radical product on the time scale of the reaction.

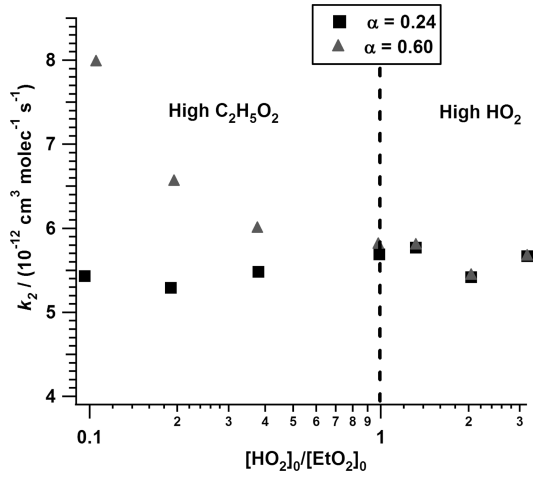

Figure 7. Dependence of k_2 on initial radical ratio at two different α's. When initial HO_2 is high the cross reaction (R2) between HO_2 and $C_2H_5O_2$ dominates so there is no effect on k_2 from the $C_2H_5O_2$ self reaction (R3) branching fraction α. At high $C_2H_5O_2$ the secondary HO_2 production controlled α becomes important, and the value for used changes the value of k_2 determined. Using $\alpha = 0.24$, determined for this particular data set, gives good agreement across all initial radical ratios unlike when using the JPL-06 recommended value.

There are a number of experimental concerns that need to be addressed when looking at the self-reaction and cross reactions of HO_2 and $C_2H_5O_2$, or any RO_2 for that matter. In the cross reaction (R2) it is important to investigate a wide range of initial radical ratios ($[HO_2]_0/[C_2H_5O_2]_0$) to test for consistency in the results. The simplest conditions to investigate (R2) are where (R3) is suppressed, i.e., at $[HO_2]_0/[C_2H_5O_2]_0 > 1$. This prevents interference due to secondary production of HO_2 from (R4), and leaves (R5) as the only competing pathway to (R2). Experiments done under the conditions of the more complicated case where $[HO_2]_0/[C_2H_5O_2]_0 < 1$, must carefully consider the secondary chemistry of (R3) and (R4). Under these conditions, measurements of k_2 also implicitly check the parameters used for (R3) due to their influence on the observed rate coefficient. Figure 2 shows the wide range of initial radical ratios examined in the current study of (R2), and the good agreement across these conditions. The initial radical ratio varied from ∼0.1 to 4 at all temperatures. This range is considerably wider than that employed in previous studies. As initial conditions shift to more $C_2H_5O_2$ and the secondary chemistry plays a larger role, the value of α used influences what value of k_2 is determined by the model. Figure 7 shows the dependence of k_2 on $[HO_2]_0/[C_2H_5O_2]_0$ and α. The data shown are the same except that the value for α used in the model fits was fixed at either the literature value of 0.60 or a value measured by this experiment of 0.24. Prior to performing the current measurement of α, we could not explain the trend observed of increasing k_2 with decreasing $[HO_2]_0/[C_2H_5O_2]_0$. The lower values for α led to a consistent value for k_2. This made it clear that previously the model was trying to compensate for too much secondary HO_2 by increasing the rate of loss of HO_2 by (R2). Table 5 lists the initial radical ratios explored by the previous temperature-dependent studies of (R2). Figure 7 shows that examining a wide range of initial radical ratios provided a useful check on the consistency of the results.

Another issue that is important to look at is the use of CH_3OH as a precursor for HO_2 in (R2). CH_3OH is a common precursor

TABLE 5: Summary of Experimental Conditions for the Determination of the $HO_2 + C_2H_5O_2$ Reaction Rate Constant

ref	technique[a]	source gases	$[CH_3OH]$[b]	bath	T[c]	P[d]	$[HO_2]_0/[EtO_2]_0$	λ_{UV}[e]
10	FP/UV	$Cl_2/O_2/C_2H_6/CH_3OH$	1.1−5.5	N_2	248−380	100	0.22−6	250
					298	25−400		
11	FP/UV	$Cl_2/O_2/C_2H_6/CH_3OH$	1.5−6	N_2	248−460	760	0.5−2.0	220
								260
12	LFP/UV	$F_2/O_2/C_2H_6/H_2$		N_2	210−363	200	1.3 (0.6−2 at 243 and 338)	
9	FP/UV/IR	$Cl_2/O_2/C_2H_6/CH_3OH$	0.06	N_2	295	2.4	2	210
								260
8	LFP/UV	H_2O_2/C_2H_6		air	298	760	0.1−0.25	210
								270
13	CIMS	$F_2/O_2/C_2H_6/H_2/He$[f]		N_2	195−298	75−200	<1	
g	LFP/UV/IR	$Cl_2/O_2/C_2H_6/CH_3OH$	0.001−0.1	O_2	221−296	100	0.3−10	250

[a] FP, flash photolysis; LFP, laser flash photolysis; CIMS, chemical ionization mass spectrometry; UV, UV absorption spectroscopy; IR, near-IR diode laser spectroscopy. [b] Units: $\times 10^{16}$ molecules cm^{-3}. [c] Units: K. [d] Units: Torr. [e] Units: nm. [f] Microwave discharge creates radicals. [g] Present work.

for HO_2, but as discussed in the results and analysis section, it is now known that CH_3OH and HO_2 form a hydrogen bonded complex at low temperatures that enhances the observed rate of the HO_2 self-reaction (R5). Previous studies that used CH_3OH as a precursor may have underestimated k_5 because the chaperone effect was not accounted for. This may have led to an overestimate of k_2 in order to fit the observed time decay of the HO_2 signal by attributing the increased decay to reaction with $C_2H_5O_2$ instead of the effect of $CH_3OH \cdot HO_2$ on (R5). In the section on comparison with previous work, it will be noted when this could be a contributing factor. This experiment did not measure a direct enhancement in the observed rate coefficient k_2 due to the $CH_3OH \cdot HO_2$ complex reacting with $C_2H_5O_2$. Therefore it is only the chaperone effect on k_5 that could cause problems.

The last experimental issue pertains to the measurement of α. This experiment is able to make the first direct measurement on the time scale of the reaction. The other studies have all relied on ratios of stable end products minutes after the reaction, which are susceptible to unknown secondary chemistry.

A. Previous work: $HO_2 + C_2H_5O_2$. Figure 4 displays all of the previous work on reaction R2 at temperatures ≤298 K. The first three temperature-dependent studies (Dagaut et al., Maricq et al., and Fenter et al.) did not agree well, motivating this study. The present work is in closest agreement with Dagaut et al.[10] As with all of the UV absorption studies, Dagaut et al. was not able to independently monitor both radicals but had to rely on spectral deconvolution. The study also only looked at two temperautures below 298 K. Three other factors that may influence the agreement between the studies are the initial radical ratio range explored, the use of CH_3OH as an HO_2 precursor, and the UV cross section used. Dagaut et al. did explore a wide range of initial radical ratios, but they were using the larger value for α recommended by the end product studies. This may have biased their results to larger values although they did not report any discrepancy in k_2 when changing initial radical ratio. They also used large values of CH_3OH ($1.1-5.5 \times 10^{16}$ molecules/cm^3) as an HO_2 precursor without accounting for the CH_3OH chaperone effect, leading to a potential overestimate of k_2 at lower temperatures. Lastly, the UV cross sections used by Dagaut et al. were lower than those currently recommended, and it is estimated that using the current recommendation would add ∼20−30% to the values reported.[3,12] It is possible that the competing errors may somewhat offset each other leading to the agreement seen.

Maricq et al.[12] is another UV absorption study in reasonable agreement with our work. The study used fluorine chemistry as a precursor for its radicals, so no correction for CH_3OH is needed. There is good agreement for the value of E_A/R across Dagaut et al., Maricq et al., and the current work. Some of the difference between the actual values in Maricq et al. and the present work can probably be attributed to larger k_2 from larger α values used because the bulk of their experiment were carried out at $[HO_2]_0/[C_2H_5O_2]_0 = 0.67$. However, the small excess of $C_2H_5O_2$ under their conditions would account for at most 5−10% of the ∼50% discrepancy. There are no other obvious reasons for the discrepancy between the experiments, but especially at low temperatures the agreement becomes better as the data sets agree within the stated uncertainties.

Fenter et al.[11] is the temperature-dependent study that deviates from the rest. It was a UV absorption study similar to the works of Maricq et al. and Dagaut et al. The low-temperature data were limited to two points below 298 K, and the study also used large CH_3OH concentrations ($(1.5-6) \times 10^{16}$ molecules/cm^3) without knowing about the chaperone effect. This effect would not be large enough to account for the discrepancy seen here. As has been stated previously, there is no clear reason for the discrepancy between the Fenter et al. results and the rest, but the additional results presented suggest there may have been a systematic error in the low temperature work. The Arrhenius parameters and k_2(298 K) of Fenter et al. stand out in Table 3.

The most recent investigation is the work of Raventos-Duran et al.,[13] which used the CIMS technique, and was published after this work was almost completed. This experiment was the only one not using UV absorption for radical detection and was the first temperature-dependent study to independently monitor the HO_2 and $C_2H_5O_2$ concentrations. The agreement between the Raventos-Duran et al. work and the current study appears acceptable especially at low temperatures. Their E_A/R value of 864 K^{-1} is moderately larger than the currently recommended value of 700 K^{-1}.

There have also been two room temperature studies by Cattell et al. and Boyd et al.[8,9] The Cattell et al. study was the first to use diode laser IR spectroscopy to independently monitor HO_2. They could not simultaneously measure HO_2 and $C_2H_5O_2$, as in the current study, but there is good agreement between our values. The Boyd et al. study used only UV absorption and is in better agreement with the Maricq et al. value at 298 K.

Overall the present work and the Raventos-Duran et al. work suggest that, of the initial temperature dependent studies on k_2, the low-temperature Fenter et al. measurements are the outliers. The largest uncertainties of k_2 remain in its 298 K value, but there is reasonable agreement in its temperature dependence and overlap within the uncertainties among lower temperature data points.

TABLE 6: Summary of Previous Experiments on $C_2H_5O_2 + C_2H_5O_2$

ref	technique[a]	source gas	T (K)	P (Torr)	λ (nm)	$\sigma^b/10^{-18}$ used[c]/rec[d]	E_a/R (K)
14	FP/UV	$(CH_3CH_2)_2N_2/O_2$	298	625	230−250 (236)	3.9/4.4	
15	MM/UV	$(CH_3CH_2)_2N_2/O_2$	303−457	495	240	6.23/4.52	
23	PR/UV	$H_2/C_2H_4/O_2$	298	760	240	5.19/4.52	
9	MM/UV	$(CH_3CH_2)_2N_2/O_2$	266−347.5	27−760	260	3.4/3.24	0
24	FP/UV	$Cl_2/C_2H_6/O_2$	228−380	25−400	250	3.89/4.12	110 ± 40
21	MM/UV	$Cl_2/C_2H_6/O_2$	218−333	760	250	4/4.12	147 ± 30[e]
11	FP/UV	$Cl_2/C_2H_6/O_2$	248−260	760	220−260 (240)	4.89/4.52	−60 ± 40
22	MM/UV	$Cl_2/C_2H_6/O_2$	253−363	200	240−250 (250)	4.04/4.12	128
20	LFP/CRDS	$Cl_2/C_2H_6/O_2$	295	5.5	270	2.14/2.14	
f	LFP/UV	$Cl_2/C_2H_6/O_2$	221−295	50−200	250	4.12/4.12	−58 ± 45

[a] FP, flash photolysis; MM, molecular modulation; PR, pulse radiolysis; LFP, laser flash photolysis; UV, UV absorption; CRDS, cavity ringdown spectroscopy. [b] Units of cm^{-2}. [c] Value of σ used in the ref to determine k_{3obs}. [d] Value of σ from JPL-06[36] that was used to normalize k_{3obs}. [e] Over the T range 250−330, below 250 curvature is observed. [f] Present work.

B. Previous work: $C_2H_5O_2 + C_2H_5O_2$: k_{3obs}. All previous investigations of reaction R3 have studied either the kinetics or the branching fraction of the reaction, but unlike this experiment, never both simultaneously. Previous kinetics measurements obtained values for k_{3obs} and then determined k_3 using α determined from end product studies and the relationship in eq 1. Figure 5 is a comparison of results for k_{3obs}. The results from this study are the largest reported values and are ∼25% larger than the JPL-06 recommended value at 298 K. We report an $E_A/R = -58$ K by fitting an Arrhenius expression to the data. Of the previous studies, The Fenter et al.[11] work ($E_A/R = -60$ K) and the Cattell et al.[9] data ($E_A/R \sim 0$) are in the closest agreement with the present study. The Fauvet et al.[22] ($E_A/R =$ 128 K) and Wallington et al.[24] ($E_A/R = 110$ K) agree very well with each other and both observe the opposite trend of a steady decrease in rate constant with temperature. Anastasi et al.[15] also observed a decreasing rate constant but with a much steeper decline than which was observed in any other study. None of the other previous studies went quite as low in temperature as Bauer et al., so it is possible that they would not have observed the change in temperature dependence observed by Bauer et al., and there is some evidence for the beginning of a change at the lowest temperature of Wallington et al. and Fauvet et al. There are no clear experimental reasons for the discrepancies between the different studies. All the studies were done using UV absorption, and the data have been normalized as best as possible for differences in σ as discussed in the results section. Table 6 summarizes the experimental conditions of each study and the measured E_A/R. Agreement between studies is not split down obvious lines of different experimental techniques, source chemistry, or pressure range. None of the previous studies saw any effect due to pressure. The overall spread in the data from the different studies would ideally be less, but is not unreasonable. However the temperature dependence of the reaction is still very uncertain, and more work to determine it is needed.

C. Previous Work: $C_2H_5O_2 + C_2H_5O_2$: k_3 and α. This experiment is the first to measure k_3 directly, and not rely on eq 1 in order to calculate it. Table 4 lists the values measured and compares them with the current recommendation.[36,39] The measured values are nearly twice the currently recommended value. This increase is predominantly due to the difference in α; the rest of the discrepancy is explained by the slightly larger values of k_{3obs} discussed above. The current recommendation lists (R3) as having no T dependence, which is in agreement with the value from this work, $E_A/R = 23 \pm 61$ K.

The current study is also the first "direct" study of α. Monitoring the HO_2 from reaction R4 is not technically a direct measurement as it is one step removed from the actual $C_2H_5O_2$ self-reaction. However under most experimental conditions, sufficient O_2 ensured essentially complete conversion by reaction R4, and the possibility of (R10) was accounted for. Every previous measurement of α was a continuous photolysis end product study which made measurements of the stable products on a time scale of minutes. Of the five previous studies on α, we will focus on three.[15,26,27] The other works by Kaiser et al.[25] and Anastasi et al.[19] were superseded by a new study from the same group and never published in the peer reviewed literature, respectively, and will not be mentioned further here. Figure 6 shows the wide gap between the current and previous measurements, this discrepancy is discussed below.

The study by Anastasi et al.[15] was a continuous photolysis experiment using azoethane ($(C_2H_5)_2N_2/O_2$) initiation chemistry and irradiation by UV lamps. They used GC/MS detection of the products over the course of minutes, and explored temperatures in the range 303−372 K. Total pressure was varied, but typically was ∼500 Torr. Product ratios were related to the reaction rates by the expressions[26]

$$[C_2H_5OH]/[CH_3CHO] = k_{3b}/(2k_{3a} + k_{3b}) \quad (4)$$

$$[C_2H_5OOH]/[C_2H_5OH] = 2k_{3a}/k_{3b} \quad (5)$$

They also explored the effect different O_2 concentrations had on the product ratios and noticed an increase in C_2H_5OOH yield and decrease in C_2H_5OH yield as O_2 is raised. This indicates that the products in reaction R10 not only may be the stable ones suggested but also may have a channel producing C_2H_5OH and a diradical (e.g., CH_3CHOO). Overall they did not observe steady product ratios over time and tried to rely on the initial rates of formation at high O_2 to determine α. In the modeling of their data they also used quite different values for key rate coefficients which could have influenced their determination of the initial rates. The combination of these effects makes it difficult to compare their results to the current study but does suggest that it is possible that the different time scales of the end product study and the current study could display very different results.

The first measurement of α was made by Niki et al.[26] using a continuous photolysis FTIR experiment at room temperature and 700 Torr. Data were typically recorded after 5, 10, or 20 min periods of irradiation by UV lamps. Both azoethane and chlorine ($Cl_2/C_2H_6/O_2$) chemistries were used to generate the radicals. Similar product ratios for $[C_2H_5OH]/[CH_3CHO]$ were found for both chemistries, and there was no change over time. A different ratio than those previously mentioned, the ratio of $[C_2H_5OOH]/[CH_3CHO]$, did appear to decrease with time, and

this decrease was more evident when using the azoethane chemistry that required longer irradiation times. They interpreted the changing ratio as a heterogeneous loss of C_2H_5OOH. One possibility of chemistry that was overlooked in this study is the reaction of Cl with C_2H_5OH.[40]

$$Cl + C_2H_5OH \rightarrow CH_3CHOH + HCl \ (\sim 90\%) \quad \text{(R14a)}$$

$$\rightarrow CH_2CH_2OH + HCl \ (\sim 10\%) \quad \text{(R14b)}$$

$$CH_3CHOH + O_2 \rightarrow HO_2 + CH_3CHO \quad \text{(R15)}$$

If this chemistry were occurring in the chlorine system, then it could provide an explanation for how over time the yield of C_2H_5OH could be artificially reduced and that of CH_3CHO increased to yield an apparently higher branching fraction in k_{3a}. Simultaneous Cl reaction with CH_3CHO at comparable rates as (R14) would keep the ratio in eq 5 stable,[41,42] as observed in their data. However this chemistry would not explain the agreement seen between the two different initiation chemistries because this chemistry would not occur in azoethane mixture where no Cl is present.

The last study by Wallington et al.[27] is very similar to the Niki et al. study and is also a continuous photolysis FTIR study. It was a room temperature study at 700 Torr total pressure. Chlorine initiation chemistry was used, and no change in the product ratios with time was observed. They note that they had the smallest surface/volume ratio of any of the previous experiments minimizing the effect of any surface reactions. The reactions of Cl with the products C_2H_5OH, CH_3CHO, and C_2H_5OOH were modeled and corrections were made to the observed product ratios, but it is not clear that the full sequence of reactions R14 and R15 are included to allow another route of production for CH_3CHO. For both the Niki et al. and Wallington et al. studies, there are no clear reasons for the discrepancy between the current results and theirs, but the time scale difference between the experiments could have allowed for secondary chemistry to interfere.

One hypothesis for secondary chemistry that could have occurred in the end product studies is photolysis of the diethylperoxide $C_2H_5O_2C_2H_5$ formed through the pathway (R3c).

$$C_2H_5O_2C_2H_5 + h\nu \rightarrow 2C_2H_5O \quad \text{(R16)}$$

Of the three studies only Niki et al. saw any evidence for its formation. If the diethylperoxide formed and photolyzed on the time scale of seconds, it would generate ethoxy radicals. The ethoxy radicals would not be distinguishable from the fraction of the reaction that proceeded through pathway R3a and would be lumped together during the end product studies.

The lower value of α measured in this study is closer to α for the CH_3O_2 self-reaction which ranges from 0.28 to 0.43.[3] However a temperature dependence is not observed for α in this study, but an experiment by Horie et al.[43] on CH_3O_2 measured a steep decrease in the k_{3a}/k_{3b} branching ratio with temperature down to 223 K. The temperature dependence of k_3 is fairly flat in the studied temperature range unlike the strong temperature dependence measured for the CH_3O_2 self-reaction rate coefficient, which could explain the difference in the temperature dependence of α between the two systems. One difficulty in making comparisons between RO_2 is the uncertainty in the mechanism of the self-reaction, which will be discussed further next. Still, given the large deviation between α measured with our experiment and the value from the end product studies in the literature, validation of these results will be necessary.

D. Mechanism. The complete picture of reaction R2 has been developed by work done on both the mechanism and products of the reaction. A number of product studies using FTIR have determined that the product channel shown for reaction R2 is the only one available at room temperature.[44−46] The Raventos-Duran et al.[13] temperature-dependent CIMS study confirmed that C_2H_5OOH is the major product channel all the way down to 195 K.[13] Work by Elrod et al. on $CH_3O_2 + HO_2$,[47] detected a minor channel leading to the products $HCHO + H_2O + O_2$ that grew larger at lower temperature. The Raventos-Duran et al. work could not check for the analogous minor channel leading to $CH_3CHO + H_2O + O_2$, and so this would be worth investigating. Recent theoretical works agree with the product studies about the dominant product channel[13,48,49] and are coming to a consensus on the likely mechanism for $RO_2 + HO_2$ reactions in general. The general mechanism involves the formation of both a hydrogen bonded intermediate on the triplet surface and a tetroxide intermediate on the singlet surface. Barriers to the transition state are too high on the singlet surface (when R is a straight chain alkyl group) despite the more stable nature of the tetroxide. The bulk of the reaction then proceeds through the hydrogen bonded structure on the triplet surface. The intermediate formation is indicative of the negative activation energy observed in the reaction's Arrhenius dependence. The lack of an observed pressured dependence on the reaction indicates that the intermediate formation is the rate-limiting step and that it proceeds to products prior to a collision. The fact that collisional stabilization is not needed prior to reaction may explain the lack of an observed enhancement in the rate of reaction R2 in the presence of the $HO_2 \cdot CH_3OH$ complex, as there is no benefit to having the CH_3OH as a collision partner.

Other HO_2 hydrogen bonded complexes have shown a similar lack of rate enhancement when reacting with RO_2. The $HO_2 \cdot H_2O$ complex has been observed, and its effect of increasing the observed rate of reaction R5 is well-known.[50−53] The large amounts of H_2O vapor in the atmosphere make the reactions of $HO_2 \cdot H_2O$ potentially very important. Recent work from English et al. showed that H_2O did not enhance the observed rate of reaction between $CH_3O_2 + HO_2$.[54] This work along with the current study provides further confirmation of the likely mechanism for the $RO_2 + HO_2$ reactions.

The mechanism of reaction R3 and the self-reaction of RO_2 in general needs more work. A recent paper by Dibble et al. summarizes the current theory and its problems.[55] The Russell mechanism for the production of the stable products through a cyclic tetroxide intermediate has been the accepted mechanism for all simple RO_2 self-reactions.[56] However, the most rigorous theoretical study on the smallest system, the CH_3O_2 self-reaction, did not find a transition state resembling the Russell mechanism pathway.[57] This raises serious questions that need to be resolved given the long-standing acceptance of the Russell mechanism. For reaction R3 specifically there has been only one computational attempt to determine the reaction pathway.[58] This study shows a transition state below the energy of the reactants for all three reaction paths (R3a, R3b, and R3c) but, in light of the analysis in the Dibble paper, may need a higher level of theory to capture the behavior observed in experiments. Furthermore, given the uncertainty now in the measured value of α, understanding the actual reaction path to the various product channels will allow a prediction of α to compare with the

experiments. Lastly, from the variation in rate coefficients, and their temperature dependences, between the CH_3O_2 and $C_2H_5O_2$ self-reactions ($\sim 4.5 \times 10^{-13}$ and $\sim 1.5 \times 10^{-13}$), it is clear that work on different examples of RO_2 are needed to understand the mechanism of the self-reaction and shed light on the variety of kinetics measured.

Conclusion

The kinetics of the $C_2H_5O_2$ reaction system, including k_2, k_{3obs}, k_3, and α, were measured using simultaneous independent detection of the $C_2H_5O_2$ and HO_2 radicals. WM NIR spectroscopy allowed for sensitive and specific detection of HO_2 while UV absorption was used to monitor $C_2H_5O_2$. The first direct measurements of k_3 and α were made, and their sensitivity to k_2 was established. Self-consistency established between all the measured parameters provided confidence in the measurements and helped determine the overall uncertainty in each. The experiments on the atmospherically important k_2 added to the growing consensus on the mechanism and overall rate constant for this reaction with an Arrhenius expression

$$k_2(T) = \left(6.01^{+1.95}_{-1.47}\right) \times 10^{-13} \exp\left(\frac{638 \pm 73}{T}\right) \text{cm}^3 \text{ molecules}^{-1} \text{ s}^{-1}$$

Meanwhile the measurements of k_3 and α provided strikingly different results than those obtained previously

$$k_3(T) = \left(1.29^{+0.34}_{-0.27}\right) \times 10^{-13} \exp\left(\frac{-23 \pm 61}{T}\right) \text{cm}^3 \text{ molecules}^{-1} \text{ s}^{-1}$$

and $\alpha = 0.28 \pm 0.06$ independent of temperature. The difference in α being especially important given that its literature value is frequently used as the branching fraction value for all RO_2 self-reactions with $R \neq CH_3$. It was also the first low temperature study of α. Both experimental and theoretical verification of k_3 and α are needed in order to better understand the self-reactions of $C_2H_5O_2$ and the self-reactions of RO_2 in general.

Acknowledgment. This research was carried out by the Jet Propulsion Laboratory, California Institute of Technology, under contract with the National Aeronautics and Space Administration (NASA). This work was supported by the NASA Upper Atmosphere Research and Tropospheric Chemistry Programs and the NASA Graduate Student Research Program (GSRP). The authors would like to thank Dave Natzic for extensive laboratory support and Dr. Lance Christensen and the Okumura group for many discussions.

Note Added after ASAP Publication. This article posted ASAP on June 4, 2010. Tables 1 and 3 have been revised. The correction version posted on June 11, 2010.

References and Notes

(1) Christensen, L. E.; Okumura, M.; Sander, S. P.; Salawitch, R. J.; Toon, G. C.; Sen, B.; Blavier, J. F.; Jucks, K. W. *Geophys. Res. Lett.* **2002**, *29*.

(2) Jacob, D. J. *Introduction to Atmospheric Chemistry*; Princeton University Press: Princeton, NJ, 1999.

(3) Tyndall, G. S.; Cox, R. A.; Granier, C.; Lesclaux, R.; Moortgat, G. K.; Pilling, M. J.; Ravishankara, A. R.; Wallington, T. J. *J. Geophys. Res., [Atmos.]* **2001**, *106*, 12157.

(4) Bonn, B.; von Kuhlmann, R.; Lawrence, M. G. *Geophys. Res. Lett.* **2004**, *31*.

(5) Kroll, J. H.; Ng, N. L.; Murphy, S. M.; Flagan, R. C.; Seinfeld, J. H. *Environ. Sci. Technol.* **2006**, *40*, 1869.

(6) Paulot, F.; Crounse, J. D.; Kjaergaard, H. G.; Kurten, A.; St Clair, J. M.; Seinfeld, J. H.; Wennberg, P. O. *Science* **2009**, *325*, 730.

(7) Rudolph, J. *J. Geophys. Res., [Atmos.]* **1995**, *100*, 11369.

(8) Boyd, A. A.; Flaud, P. M.; Daugey, N.; Lesclaux, R. *J. Phys. Chem. A.* **2003**, *107*, 818.

(9) Cattell, F. C.; Cavanagh, J.; Cox, R. A.; Jenkin, M. E. *J. Chem. Soc., Faraday Trans. 2* **1986**, *82*, 1999.

(10) Dagaut, P.; Wallington, T. J.; Kurylo, M. J. *J. Phys. Chem.* **1988**, *92*, 3836.

(11) Fenter, F. F.; Catoire, V.; Lesclaux, R.; Lightfoot, P. D. *J. Phys. Chem.* **1993**, *97*, 3530.

(12) Maricq, M. M.; Szente, J. J. *J. Phys. Chem.* **1994**, *98*, 2078.

(13) Raventos-Duran, M. T.; Percival, C. J.; McGillen, M. R.; Hamer, P. D.; Shallcross, D. E. *Phys. Chem. Chem. Phys.* **2007**, *9*, 4338.

(14) Adachi, H.; Basco, N. *Chem. Phys. Lett.* **1979**, *64*, 431.

(15) Anastasi, C.; Waddington, D. J.; Woolley, A. *J. Chem. Soc., Faraday Trans.* **1983**, *79*, 505.

(16) Andersson, B. Y.; Cox, R. A.; Jenkin, M. E. *Int. J. Chem. Kinet.* **1988**, *20*, 283.

(17) Tang, Y. X.; Tyndall, G. S.; Orlando, J. J. *J. Phys. Chem. A.* **2010**, *114*, 369.

(18) Stone, D.; Rowley, D. M. *Phys. Chem. Chem. Phys.* **2005**, *7*, 2156.

(19) Anastasi, C. B. M. J.; Smith, D. B.; Waddington, D. J. Joint Meeting of the French and Italian Sections of the Combustion Institute, June 1987, Amalfi.

(20) Atkinson, D. B.; Hudgens, J. W. *J. Phys. Chem. A* **1997**, *101*, 3901.

(21) Bauer, D.; Crowley, J. N.; Moortgat, G. K. *J. Photochem. Photobiol., A* **1992**, *65*, 329.

(22) Fauvet, S.; Ganne, J. P.; Brion, J.; Daumont, D.; Malicet, J.; Chakir, A. *J. Chim. Phys. Phys.-Chim. Biol.* **1997**, *94*, 484.

(23) Munk, J.; Pagsberg, P.; Ratajczak, E.; Sillesen, A. *J. Phys. Chem.* **1986**, *90*, 2752.

(24) Wallington, T. J.; Dagaut, P.; Kurylo, M. J. *J. Photochem. Photobiol., A* **1988**, *42*, 173.

(25) Kaiser, E. W.; Rimai, L.; Wallington, T. J. *J. Phys. Chem.* **1989**, *93*, 4094.

(26) Niki, H.; Maker, P. D.; Savage, C. M.; Breitenbach, L. P. *J. Phys. Chem.* **1982**, *86*, 3825.

(27) Wallington, T. J.; Gierczak, C. A.; Ball, J. C.; Japar, S. M. *Int. J. Chem. Kinet.* **1989**, *21*, 1077.

(28) Lightfoot, P. D.; Cox, R. A.; Crowley, J. N.; Destriau, M.; Hayman, G. D.; Jenkin, M. E.; Moortgat, G. K.; Zabel, F. *Atmos. Environ., Part A* **1992**, *26*, 1805.

(29) Christensen, L. E.; Okumura, M.; Sander, S. P.; Friedl, R. R.; Miller, C. E.; Sloan, J. J. *J. Phys. Chem. A* **2004**, *108*, 80.

(30) Kaiser, E. W. *J. Phys. Chem.* **1995**, *99*, 707.

(31) Clifford, E. P.; Farrell, J. T.; DeSain, J. D.; Taatjes, C. A. *J. Phys. Chem. A* **2000**, *104*, 11549.

(32) Kaiser, E. W.; Lorkovic, I. M.; Wallington, T. J. *J. Phys. Chem.* **1990**, *94*, 3352.

(33) DeSain, J. D.; Ho, A. D.; Taatjes, C. A. *J. Mol. Spectrosc.* **2003**, *219*, 163.

(34) *FACSIMILE, 4.0.36 ed.*; MCPA Software Ltd., 2002.

(35) Thiebaud, J.; Crunaire, S.; Fittschen, C. *J. Phys. Chem. A* **2007**, *111*, 6959.

(36) Sander, S. P.; Finlayson-Pitts, B. J.; Friedl, R. R.; Golden, D. M.; Huie, R. E.; Kolb, C. E.; Kurylo, M. J.; Molina, M. J.; Moortgat, G. K.; Orkin, V. L.; Ravishankara, A. R. *JPL 2006: Chemical Kinetics and Photochemical Data for Use in Atmospheric Studies*; Evaluation No. 15, JPL Publication 06-2, 2006, Jet Propulsion Lab, 2006.

(37) Vaghjiani, G. L.; Ravishankara, A. R. *J. Chem. Phys.* **1990**, *92*, 996.

(38) Christensen, L. E.; Okumura, M.; Hansen, J. C.; Sander, S. P.; Francisco, J. S. *J. Phys. Chem. A.* **2006**, *110*, 6948.

(39) Atkinson, R.; Baulch, D. L.; Cox, R. A.; Crowley, J. N.; Hampson, R. F.; Hynes, R. G.; Jenkin, M. E.; Rossi, M. J.; Troe, J. *Atmos. Chem. Phys.* **2006**, *6*, 3625.

(40) Taatjes, C. A.; Christensen, L. K.; Hurley, M. D.; Wallington, T. J. *J. Phys. Chem. A* **1999**, *103*, 9805.

(41) Wallington, T. J.; Skewes, L. M.; Siegl, W. O.; Wu, C. H.; Japar, S. M. *Int. J. Chem. Kinet.* **1988**, *20*, 867.

(42) Seakins, P. W.; Orlando, J. J.; Tyndall, G. S. *Phys. Chem. Chem. Phys.* **2004**, *6*, 2224.

(43) Horie, O.; Crowley, J. N.; Moortgat, G. K. *J. Phys. Chem.* **1990**, *94*, 8198.

(44) Hasson, A. S.; Tyndall, G. S.; Orlando, J. J. *J. Phys. Chem. A* **2004**, *108*, 5979.

(45) Spittler, M.; Barnes, I.; Becker, K. H.; Wallington, T. J. *Chem. Phys. Lett.* **2000**, *321*, 57.

(46) Wallington, T. J.; Japar, S. M. *Chem. Phys. Lett.* **1990**, *166*, 495.

(47) Elrod, M. J.; Ranschaert, D. L.; Schneider, N. J. *Int. J. Chem. Kinet.* **2001**, *33*, 363.

(48) Hasson, A. S.; Kuwata, K. T.; Arroyo, M. C.; Petersen, E. B. *J. Photochem. Photobiol., A* **2005**, *176*, 218.
(49) Hou, H.; Li, J.; Song, X. L.; Wang, B. S. *J. Phys. Chem. A* **2005**, *109*, 11206.
(50) Aloisio, S.; Francisco, J. S.; Friedl, R. R. *J. Phys. Chem. A* **2000**, *104*, 6597.
(51) Kanno, N.; Tonokura, K.; Tezaki, A.; Koshi, M. *J. Phys. Chem. A* **2005**, *109*, 3153.
(52) Kircher, C. C.; Sander, S. P. *J. Phys. Chem.* **1984**, *88*, 2082.
(53) Suma, K.; Sumiyoshi, Y.; Endo, Y. *Science* **2006**, *311*, 1278.
(54) English, A. M.; Hansen, J. C.; Szente, J. J.; Maricq, A. M. *J. Phys. Chem. A* **2008**, *112*, 9220.
(55) Dibble, T. S. *Atmos. Environ., Part A* **2008**, *42*, 5837.
(56) Russell, G. A. *J. Am. Chem. Soc.* **1957**, *79*, 3871.
(57) Ghigo, G.; Maranzana, A.; Tonachini, G. *J. Chem. Phys.* **2003**, *118*, 10575.
(58) Feria, L.; Gonzalez, C.; Castro, M. *Int. J. Quantum Chem.* **2004**, *96*, 380.

JP912129J